C2012-0001728

Chloride Threshold Dependence on Potential in Reinforced Mortar

Andrea N. Sánchez and Alberto A. Sagüés
University of South Florida
Department of Civil and Environmental Engineering
4202 East Fowler Ave.
Tampa, FL 33620 U.S.A.

ABSTRACT

Additional assessment of the chloride threshold dependence on steel potential is presented to supplement the limited set of available data. Cylindrical mortar specimens with an embedded steel rebar were exposed to NaCl saturated solution under potentiostatic control at open circuit potential and -200, -400 and -600 mV vs. saturated calomel electrode (SCE). Once corrosion started, the specimens were demolished and the chloride content at the rebar surface was determined and reported as the chloride threshold (C_T) for that condition. The present results tend to agree with those of previous investigators showing that negative polarization of several hundred mV may be needed to attain an increase in corrosion initiation threshold of about one order of magnitude. An updated survey of the literature is consistent with the lower bound of that beneficial effect being approximately described by a threshold value in the order of 0.5% by weight of cement at E=-100 mV (SCE), with a negative slope provisionally in the order of ~550 mV per decade of chloride content.

Key words: potential, chloride corrosion threshold, service life, potential, steel.

©2012 by NACE International. Requests for permission to publish this manuscript in any form, in part or in whole, must be in writing to NACE International, Publications Division, 1440 South Creek Drive, Houston, Texas 77084. The material presented and the views expressed in this paper are solely those of the author(s) and are not necessarily endorsed by the Association.

INTRODUCTION

Reinforced concrete in marine and deicing salt service experiences corrosion due to the ingress of chloride ions. Corrosion initiates once the concentration of chloride ions at the steel surface reaches a minimum required amount, defined as the chloride corrosion threshold, C_T. This is a key parameter for long term prediction of reinforced concrete structures.[1] The value of C_T depends on many variables such as the condition of the steel surface and concrete properties, as well as the potential of the steel while in the passive state.[2] This last factor has received relatively little attention in the literature. A previous review by Presuel-Moreno et al. noted that the general trends from a broad set of data from multiple studies followed the pattern recognized in systematic investigations by Alonso whereby C_T increases when potentials are more cathodic than -200±50 mV (SCE) and is relatively independent of the potential when it is more anodic than that value.[3,4] The increase with cathodic polarization followed an exponential dependence with $\log_{10}C_T \sim k - E / 0.4V$ where k is a constant and E the potential, a relationship that resembles as expected that between pitting potential and chloride content in pitting corrosion.[5] Those trends were however, obtained from limited test conditions involving a small area of steel (6 cm^2, 0.9 sq. inch.) beneath a thin mortar cover (0.5 cm., 0.2 inch.), conditions that tend to add uncertainty to the values of C_T obtained.[6] Given those limitations and the overall scarcity of applicable data, experiments have been initiated to provide additional assessment of the chloride threshold dependence on steel potential, in particular allowing for chloride buildup to take place by transport through a thicker cementitious material layer and using a greater rebar exposure area. To that end, steel bars were embedded in initially chloride-free mortar cylindrical specimens immersed in a chloride rich solution. The bars were polarized to various potentials. When corrosion started at each rebar the specimen was demolished and the chloride concentration at the rebar trace was determined. The resulting threshold concentration was correlated with the polarization potential.

EXPERIMENTAL PROCEDURE

Cylindrical mortar specimens with an embedded type #5 (diameter: 1.6 cm, 0.63 inch.) rebar were submerged in a saturated NaCl (5.33 M) solution, as shown in Figure 1.[7] Plain A-615 rebar with high temperature mill scale on the surface was used.[8] The top and bottom of the rebar was coated with an epoxy resin, to prevent corrosion initiation in these areas. Ordinary Portland Cement Type I/II was used with a water-cement ratio (w/c) of 0.6 and a cement- sand ratio (c/s) of 1/3. The cement factor (CF) was 488 kg/m^3 (813 pcy). The average cover thickness of the rebar was 1.6 cm (0.6 inch.) and an exposed area of 32 cm^2 (5 sq. inch.). An embedded activated titanium reference electrode, periodically calibrated with respect to the SCE, was used for potential control in each specimen.[9] The specimens were cured for 7 days at high humidity before being placed in the exposure container. One set of duplicate specimens was exposed at the open circuit potential (OCP) and three other sets were cathodically polarized at -200, -400 and -600 mV (SCE), respectively. The solution had also addition of $Ca(OH)_2$ in excess of its solubility limit to maintain an average pH of ~>12 and minimize alkaline leaching from the mortar. A tight lid minimized access of external air and CO_2 to the solution, but sufficient oxygen existed in the container for the solution to be considered as being naturally aerated. A multiple potentiostat was used to adjust the potential for the polarized specimens and periodically corrected as needed to stay within ±10 mV of the target value. The experiment was conducted in a climate controlled laboratory with an average temperature of 21ºC (70ºF). Potential and current demands for the polarized specimens were

©2012 by NACE International. Requests for permission to publish this manuscript in any form, in part or in whole, must be in writing to NACE International, Publications Division, 1440 South Creek Drive, Houston, Texas 77084. The material presented and the views expressed in this paper are solely those of the author(s) and are not necessarily endorsed by the Association.

monitored regularly. Electrochemical Impedance Spectroscopy (EIS) measurements in the range 1mHz to 1MHz with 10 mV rms amplitude were performed periodically with a Gamry(1) 2006 device on the OCP specimens, at the OCP.

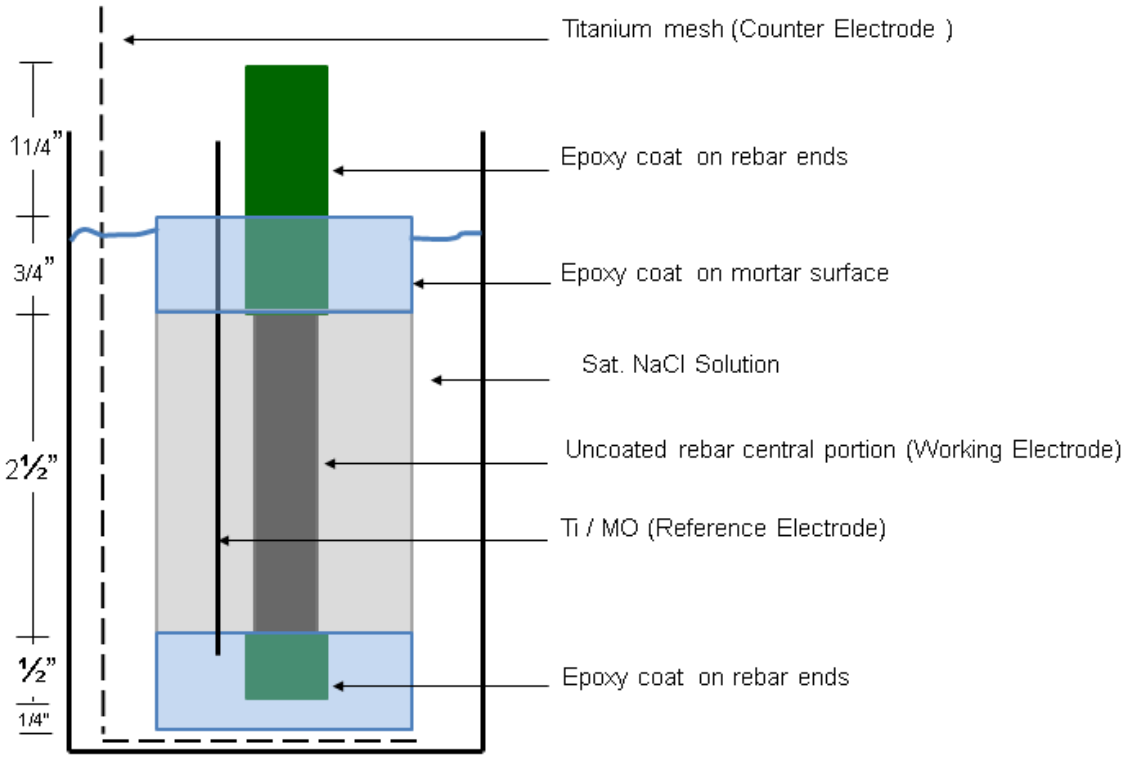

Figure 1: Specimen layout

Supplemental Test

While developing the main test procedure, an earlier series of tests were conducted with a limited number of specimens made with 0.5 w/c mortar and a CF=513 kg/m^3, and exposed to a solution with NaCl content changed stepwise from 0.5 M (day 0) to 1 M (day 36 on). Methodology was otherwise similar as the one mentioned before. Four specimens of these series experienced activation during the test period and the results are noted together with those of the present experiments.

RESULTS AND DISCUSSION

Estimation of the time of activation

For the OCP specimens the time of activation (t_A) or time when corrosion starts was estimated by observation of the potential evolution and the EIS trends shown in Figure 2a) and 2b). The Nyquist plots suggest that the interfacial EIS behavior approximated that of simple constant phase element (CPE) – polarization resistance (Rp) parallel combination. At short exposure times the value of Rp was large but later on there was a sharp transition to smaller values indicative of the onset of active corrosion. The OCP downward trend was consistent with that

(1) Trade name.

©2012 by NACE International. Requests for permission to publish this manuscript in any form, in part or in whole, must be in writing to NACE International, Publications Division, 1440 South Creek Drive, Houston, Texas 77084. The material presented and the views expressed in this paper are solely those of the author(s) and are not necessarily endorsed by the Association.

behavior. From observation of Figure 2c), the transitions took place at around the time that the OCP reached -300 mV (SCE), so that exposure duration (13 and 24 days for specimens 7 and 8, respectively) was declared to correspond to the corrosion initiation event for the present purposes.

As shown in Figure 3 the polarized specimens initially demanded cathodic currents commensurate with the extent of cathodic polarization imposed. As time progressed the absolute value of the cathodic current in the -200 and -400 mV (SCE) specimens decreased appreciably, indicative of the onset of diffusion-polarized regimes for those cases. Current demand was very small for the specimens polarized to -200 mV (SCE), which are likely to have remained near activation-polarized conditions for the cathodic reaction.

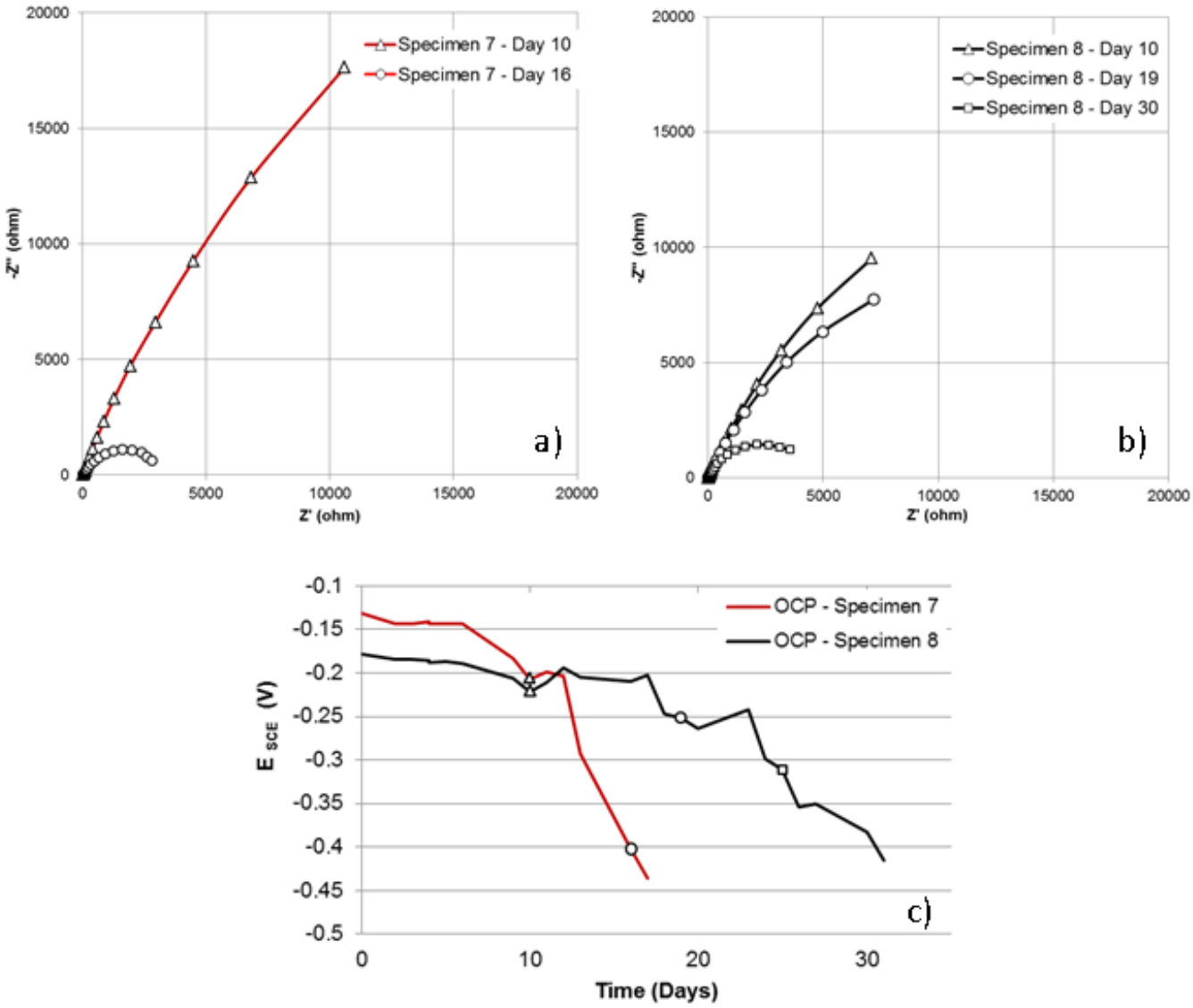

Figure 2: Time trends for OCP specimens. a),b): Nyquist diagrams (lowest frequency shown 1 mHz; 5 data per frequency decade) keyed to symbols in OCP graphs. c): Potential evolution.

©2012 by NACE International. Requests for permission to publish this manuscript in any form, in part or in whole, must be in writing to NACE International, Publications Division, 1440 South Creek Drive, Houston, Texas 77084. The material presented and the views expressed in this paper are solely those of the author(s) and are not necessarily endorsed by the Association.

Activation was manifested for the polarized specimens by a shift in the polarizing current from a cathodic to an anodic regime. Reaching an anodic current greater than 0.2 μA/cm^2 was chosen as the criterion for the onset of the active regime, following the criterion used by Alonso et al.[4] Figure 3 shows the transitions for the polarized specimens that experienced activation during the exposure period.

Specimens that underwent activation were kept in the solution for some time afterwards to confirm that the criterion was satisfied in a sustained manner, and then removed and demolished for direct assessment.

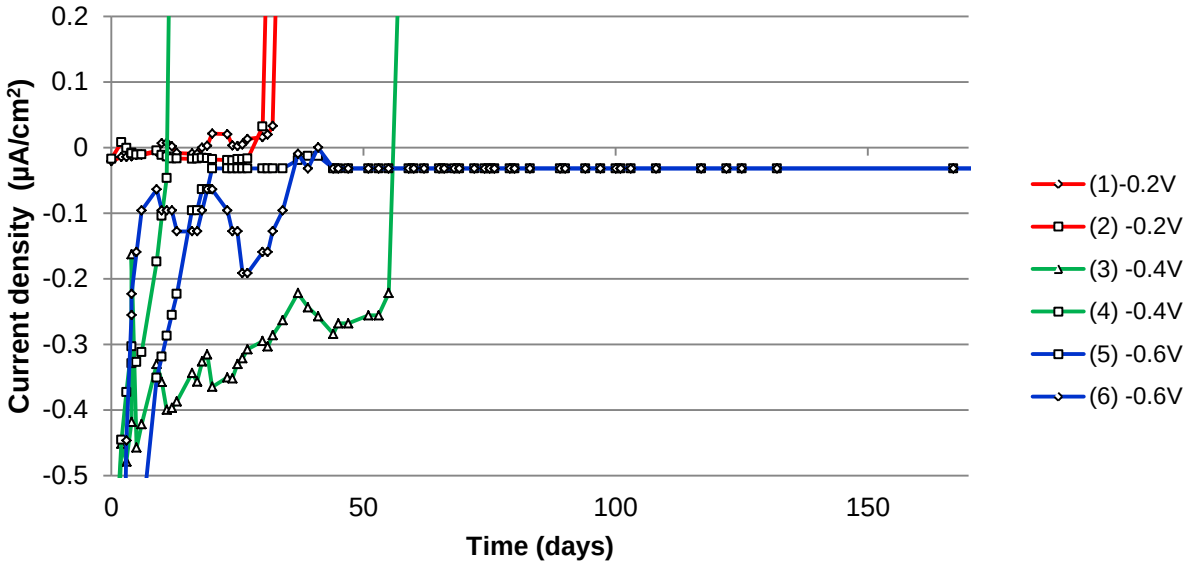

Figure 3: Applied current density (anodic is >0) vs time for each polarized specimen at the indicated potential.

After demolition a 1 cm (0.38 inch.) masonry drill was used to obtain mortar samples at the rebar trace for chloride analysis. Figure 4 illustrates the pattern of mortar powder collection from the trace of the rebar, with drillings to a depth of ~ 1 to 2 mm. Acid-soluble chloride concentration of mortar powder samples duplicates for each specimen was determined following the "Florida Method of Test for Determining Low-Levels of Chloride in Concrete and Raw Materials".[10] The chloride concentration values were expressed in the form of total chloride content by weight of cement. All the activated specimens presented localized corrosion on the rebar surface as illustrated in Figure 5.

Figure 4: Drilled holes for the mortar collection at the rebar trace (scale in inches).

©2012 by NACE International. Requests for permission to publish this manuscript in any form, in part or in whole, must be in writing to NACE International, Publications Division, 1440 South Creek Drive, Houston, Texas 77084. The material presented and the views expressed in this paper are solely those of the author(s) and are not necessarily endorsed by the Association.

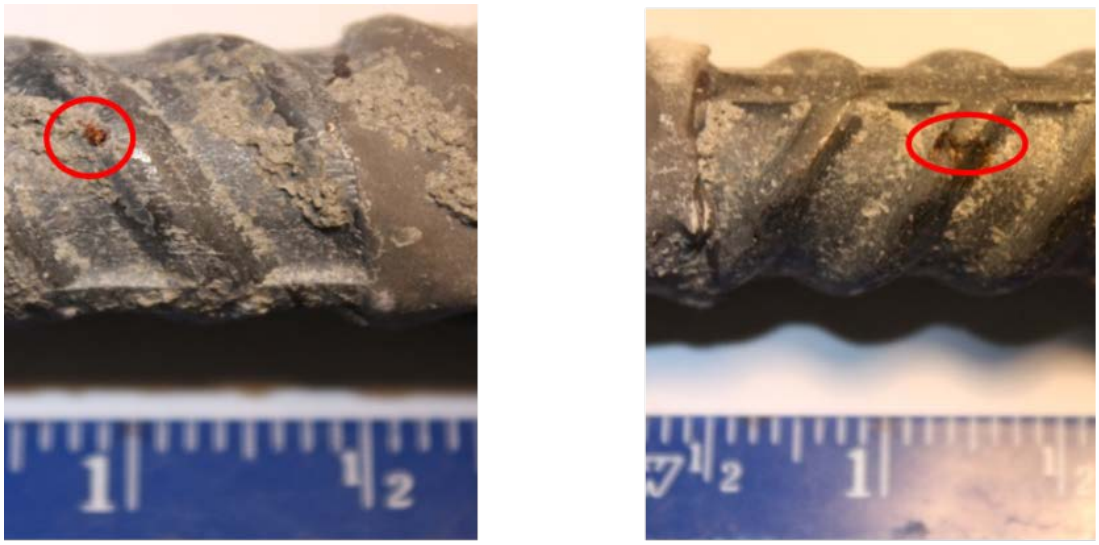

Figure 5: Localized corrosion on the rebar surface (scale in inches).

Estimation of chloride content at the rebar at the time of corrosion

Because of the confirmatory time lag between the time of specimen activation and that of extraction, the chloride content at the time of sampling of the rebar trace was usually greater than upon activation. A correction procedure was developed by assuming on first approximation simple cylindrical diffusion ruled by Equation (1) with time and space invariant apparent chloride diffusion coefficient (D), radial dimension r and time t.[11]

$$\frac{\partial C}{\partial t} = \frac{1}{r}\frac{\partial}{\partial r}\left(rD\frac{\partial C}{\partial r}\right) \quad (1)$$

The boundary conditions assumed a constant surface chloride concentration (C_S) at the outer cylinder wall and a zero-flux condition at the rebar surface, thus accounting for the rebar obstruction effect for chloride accumulation at the rebar trace.[12] The solution of Eq. (1) was solved by the Finite Difference Method (FDM). The equation was formulated in terms of dimensionless expressions: $P=Dt/a^2$, C_R/C_S and r/a; where C_R and a are chloride concentration at the rebar trace at a specific time and radius of the specimen, respectively. The output to the problem was the numerical functional relationship between C_R/C_S and P.

A representative value of C_S was obtained following a similar procedure as for the rebar trace, but sampling instead the outer cylinder surface. Samples of the outer surface of specimens 5 and 6 were analyzed yielding values respectively of 41 kg/m^3 and 40 kg/m^3, average 40.5 kg/m^3. This value is generally consistent with the expected high porosity of the mortar given its high w/c ratio, and an assumption of pores near the surface filled with the saturated NaCl solution plus some extent of chloride binding by the surrounding matrix.[13,14] The chloride content measured by chemical analysis at the rebar trace (C_{RTE}) at the time of extraction (t_E) was then divided by C_S to obtain C_{RTE}/C_S which in turn yielded $P(t_E)$ (P at the t_E) per the functional relationship determined above. With the values of t_E, $P(t_E)$ and a an estimate of D

©2012 by NACE International. Requests for permission to publish this manuscript in any form, in part or in whole, must be in writing to NACE International, Publications Division, 1440 South Creek Drive, Houston, Texas 77084. The material presented and the views expressed in this paper are solely those of the author(s) and are not necessarily endorsed by the Association.

was obtained, which was then used to obtain $P(t_A)$ and from it similarly obtain an estimate of C_{RTA}, the concentration at time of activation which is the reported threshold value.

For specimens 5 and 6, as of day >170 no activation events were observed. A lower bound for rebar trace chloride concentration was estimated by assuming that the value of D was the same as the average, 2.43 10^{-7} cm^2/s, of the rest of the specimens and using the C_R/C_S – P relationship to estimate C_{RTA} at the latest exposure time. For that long exposure, the resulting C_T value was nearly equal to the C_S value.

For the specimens from the supplemental tests (S2, S4, S7, S8), only activation time data were available. A rough estimate of C_T was made nevertheless in those cases by a similar procedure as used for specimens 5 and 6. Nominal values of C_S and D were assigned as follows. The surface concentration was assumed for simplicity (neglecting adjustments for porosity and chloride binding differences) as being directly proportional to the solution chloride content, prorating directly from the C_S value used for the main sequence tests, and further using a constant nominal weighted value based on the fraction of t_A spent in the 0.5 M and 1 M regimes. Since in the supplemental tests a 0.5 w/c mixture had been used, the corresponding value of D was estimated from the average value from the main test sequence, and multiplying it by the average ratio of D (0.5 w/c) to D (0.6 w/c) obtained from work by previous authors.[15-17]

Table 1.
Calculations and results for each test condition.

Specimen	Potential (V)	t_A (d)	t_E (d)	C_{RTE} (kg/m^3)	C_S (kg/m^3)	C_{RTE}/C_S	$P(t_E)$	D (cm^2/s)	$P(t_A)$	C_{RTA}/C_S	C_{RTA} (kg/m^3)	C_{RTA} (% wt. ct.)
1	-0.2	34	45	9.47	A	0.23	8.25E-02	1.37E-07	0.06*	0.13*	5.4*	1.10*
2	-0.2	31	31	4.00	A	0.10	5.63E-02	1.35E-07	0.06*	0.10*	4.0*	0.83*
3	-0.4	59	60	15.31	A	0.38	1.13E-01	1.40E-07	0.11*	0.37*	15*	3.06*
4	-0.4	12	13	14.03	A	0.35	1.06E-01	6.09E-07	0.11*	0.32*	13*	2.62*
5	-0.6	>170	>170	-	A	-	-	B	0.56**	0.98**	>40**	>8.1**
6	-0.6	>170	>170	-	A	-	-	B	0.56**	0.98**	>40**	>8.1**
7	-0.15	13	17	5.34	A	0.13	6.25E-02	2.75E-07	0.05*	0.06*	2.5*	0.52*
8	-0.19	24	31	6.68	A	0.16	6.88E-02	1.66E-07	0.05*	0.08*	3.4*	0.69*
S2	-0.2	117	-	-	6.5	-	-	C	0.24**	0.8**	5**	1**
S4	-0.4	152	-	-	6.7	-	-	C	0.32**	0.9**	6**	1.1**
S7	-0.12	51	-	-	5	-	-	C	0.11**	0.3**	1.7**	0.3**
S8	-0.09	63	-	-	5.5	-	-	C	0.13**	0.5**	2.5**	0.5**

Notes:
[A] Group value C_S=40.5 kg/m^3 from data for specimens 5 and 6.
[B] Estimated diffusion coefficient 2.43E-07 cm^2/s = average of values from specimens 1-4 and 7-8.
[C] Estimated diffusion coefficient 1.56E-7 cm^2/s = value obtained from the conversion of D at w/c 0.6 to D w/c 0.5, as described in text.
* Corrected from direct measurement to account for time lag between activation and extraction.
** Values obtained indirectly as explained in text.
Roundoff applied to finished values; internal table computations conducted with additional digits.

©2012 by NACE International. Requests for permission to publish this manuscript in any form, in part or in whole, must be in writing to NACE International, Publications Division, 1440 South Creek Drive, Houston, Texas 77084. The material presented and the views expressed in this paper are solely those of the author(s) and are not necessarily endorsed by the Association.

Present findings and prior C_T data

Table 1 summarizes the results and calculations of each test condition. The values for D estimated from the main test sequence were generally high, consistent with those expected for high w/c mortar in a wet environment.[15-17] It is noted that the estimated value of D for specimen 4 was significantly higher than the others, reflecting the high chloride content measured at the rebar trace of that specimen after a relatively short exposure period and the consequent early activation as well. It is speculated that mortar consolidation may have been poorer in that sample, although there was no readily visible sign of deficiency. Regardless of the early chloride buildup, the results for this specimen nevertheless followed the same overall trends discussed next. It is also recognized that the results from the supplemental tests represent only rough estimates, provided here primarily for completeness.

Figure 6 summarizes all the findings from the present experiments (red) with the addition of prior observations.[3,4,18-20] Blue symbols correspond to data from other sources published since the previous version of this figure was presented by Presuel-Moreno et al.[3] The present findings, while qualified as stated earlier especially for the supplemental tests, are generally consistent with the overall body of evidence and support the expectation of a substantial increase in threshold as the impressed potential becomes more negative. The recently added results from this work and others still support a lower bound of the beneficial effect of cathodic polarization consistent with that identified earlier, shown by the dashed line starting at E=-100 mV and C_T=0.5% with a negative slope of ~ 550 mV/decade.[3,4] Some of the C_T values determined in the present work, especially at the more negative potentials, are to the right of those obtained by Alonso et al. Additional experiments are in progress to establish whether that pattern is maintained. Nevertheless, because of the increasing number of lower bound estimates with high C_T values at the more negative potentials, the use of a more optimistic downward slope (e.g. ~-400 mV) may merit future consideration.

It is also noted that the potential effect on C_T implied by Figure 6 is figured generally on the actual concentration of chloride ions at the steel-concrete interface at the time of activation. Additional benefit is derived from any migration effect that the electric field used to apply cathodic polarization through the concrete may have in slowing down chloride ion buildup at the steel surface.[21] For a given steel polarization level that extrinsic effect varies depending on factors such as the conductivity of the concrete and should be evaluated separately. Similarly, the cathodic reaction increases local alkalinity at the steel surface, which is expected to be a factor in elevating the effective value of the threshold.[22] The extent to which that factor is responsible for the overall increase in threshold is likely to depend on cement composition and electrokinetic effects that vary with individual conditions, and it too requires additional investigation.

©2012 by NACE International. Requests for permission to publish this manuscript in any form, in part or in whole, must be in writing to NACE International, Publications Division, 1440 South Creek Drive, Houston, Texas 77084. The material presented and the views expressed in this paper are solely those of the author(s) and are not necessarily endorsed by the Association.

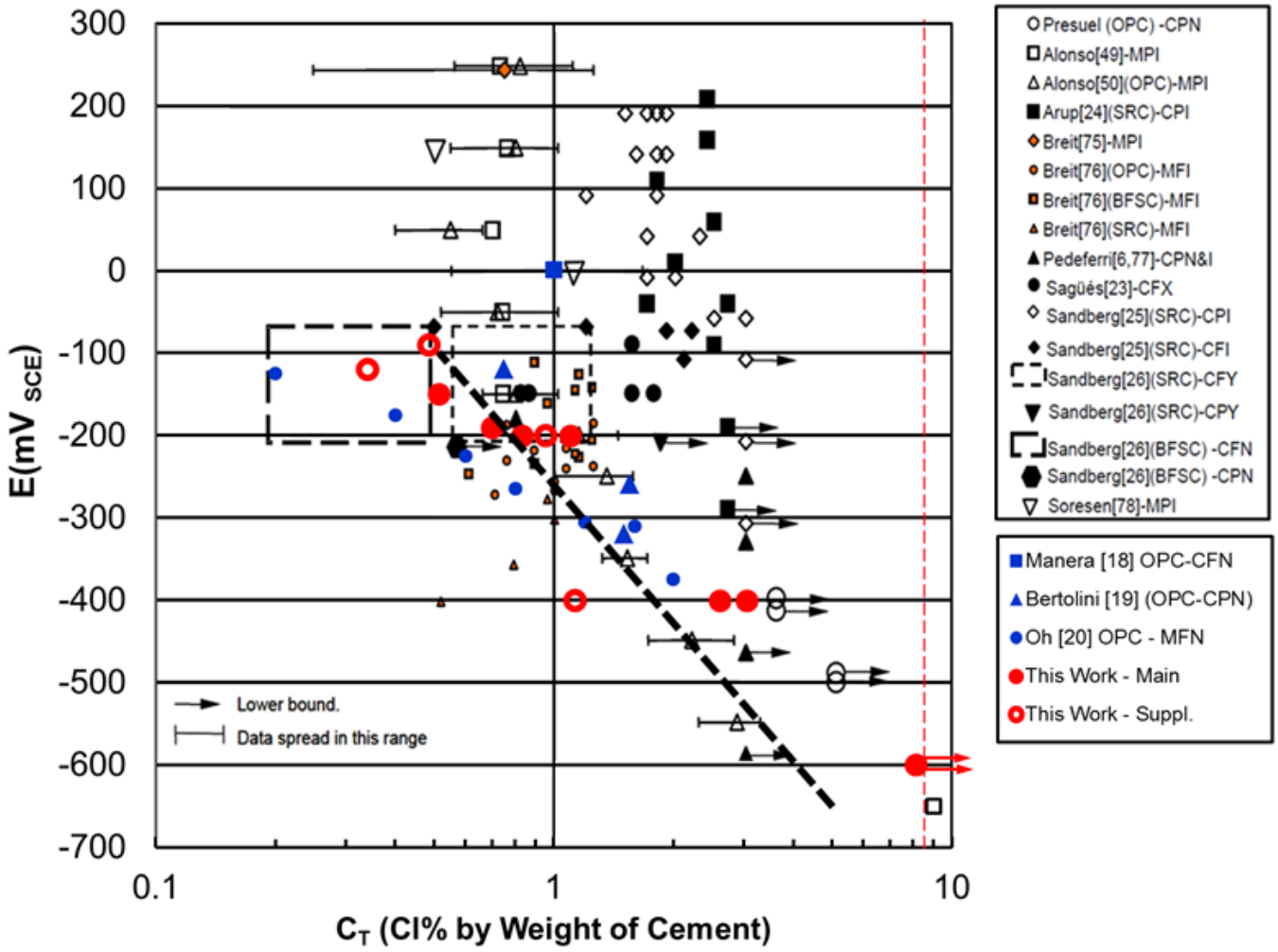

Figure 6: Chloride Threshold vs Potential. Initial compilation by Presuel-Moreno et al.[3] (black symbols); update in other sources (blue). This work in red; solid circles: main sequence; open circles: supplemental tests. Dashed line: see text. Notation: OPC: Ordinary Portland Cement; SRC: Sulfate resistant cement; BFSC: Blast furnace slag cement; M: mortar or C: concrete; P: Polarized or F: free open circuit potential; I: Immersed or N: Not Immersed; X: cyclic or permanent ponding; Y: splash zone or Z: simulated splash zone). Missing designations indicate information not available or multiple conditions. References in square brackets for the black symbols are listed in the original publication.[3]

CONCLUSIONS

- The present results tend to agree with those of previous investigators showing that negative polarization of several hundred mV may be needed to attain an increase in corrosion initiation threshold of about one order of magnitude.

- An updated survey of the literature including this work is consistent with the lower bound of that beneficial effect being approximately described by a threshold value in the order of 0.5% by weight of cement at E=-100 mV (SCE), with a negative slope of ~550 mV per decade of chloride content, possibly revisable to a less pronounced

©2012 by NACE International. Requests for permission to publish this manuscript in any form, in part or in whole, must be in writing to NACE International, Publications Division, 1440 South Creek Drive, Houston, Texas 77084. The material presented and the views expressed in this paper are solely those of the author(s) and are not necessarily endorsed by the Association.

value. Extrinsic effects, such as an electro kinetic slowdown of chloride buildup at the steel upon cathodic polarization require separate consideration.

ACKNOWLEDGEMENT

This investigation was partially supported by the Florida Department of Transportation. The opinions and findings stated here are those of the authors and not necessarily those of the funding agency. The authors would like to thank Dr. Kingsley Lau for his valuable suggestions.

REFERENCES

1. A. A. Sagüés, S.C. Kranc, and K. Lau. "Service Life Forecasting for Reinforced Concrete Incorporating Potential-Dependent Chloride Threshold", NACE Corrosion 2009, Paper No. 09213, 22 pp., NACE International, Houston, 2009.

2. U. Angst, B. Elsener, C. Larsen, Ø. Vennesland. (2009). Critical chloride content in reinforced concrete - A review.. Cement and Concrete Research, Vol. 39, issue 12, pp. 1122-1138.

3. F.J. Presuel-Moreno, A.A. Sagüés, S.C. Kranc. (2005). Steel Activation in Concrete Following Interruption of Long-Term Cathodic Polarization. Corrosion, Vol. 61, issue 5, pp. 428-436.

4. C. Alonso, M. Castellote and C. Andrade. (2002). Chloride threshold dependence of pitting potential of reinforcements. Electrochimica Acta, Vol. 47. pp. 3469-3481.

5. Z. Szlarska-Smialowska: "Pitting Corrosion of Metals", NACE International, Houston, 1986.

6. L. Li, A.A. Sagüés. (2004). Chloride Corrosion Threshold of Reinforcing Steel in Alkaline Solutions - Effect of Specimen Size. Corrosion, Vol. 60, issue 2, pp. 195-202.

7. R. Weast. CRC Handbook of Chemistry and Physics 54th Edition, Chemical Rubber Company, Cleveland, 1973.

8. A.A. Sagüés, K. Lau, A. Accardi, Final Report “Mechanistic Issues on Corrosion Performance of Dual Polymer–Zinc Coated Rebar”, Gerdau - Ameristeel, 2010.

9. P. Castro, A.A. Sagüés, E.I. Moreno, L. Maldonado, and J. Genesca. (1996). Characterization of Activated Titanium Solid Reference Electrodes for Corrosion Testing of Steel in Concrete. Corrosion, Vol. 52, issue 8, pp. 609-617.

10. Florida Method of Test for Determining Low-Levels of Chloride in Concrete and Raw Materials” (FM 5-516). Florida Department of Transportation. 2009.

11. J. Crank, The Mathematics of Diffusion, 2nd Edition, Clarendon Press, Oxford 2004.

12. S.C. Kranc, A.A. Sagüés and F.J. Presuel-Moreno. (2002). Decreased Corrosion Initiation Time of Steel in Concrete due to Reinforcing Bar Obstruction of Diffusional Flow. ACI Materials Journal, Vol. 99, issue 1, pp. 51-53.

©2012 by NACE International. Requests for permission to publish this manuscript in any form, in part or in whole, must be in writing to NACE International, Publications Division, 1440 South Creek Drive, Houston, Texas 77084. The material presented and the views expressed in this paper are solely those of the author(s) and are not necessarily endorsed by the Association.

13. Q. Yuan, C. Shi, G. De Schutter, K. Audenaert and D. Deng. (2009). Chloride binding of cement-based materials subjected to external chloride environment – A review. Construction and Building Materials, Vol. 23, pp. 1-13.

14. M.G. Hernández, M.A.G Izquierdo, M., A. Ibáñez, J.J. Anaya and L.G. Ullate. (2000). Porosity estimation of concrete by ultrasonic NDE. Ultrasonics, Vol. 38, pp. 531-533.

15. T. Oshiro and S. Tanigawa. Effect of Surface Coating on the Durability of Concrete Exposed to Marine Environment. Second International Conference Concrete in Marine Environment Proceedings, St. Andrews by-the-Sea, Canada. ACI SP109-09, pp. 179-198. American Concrete Institute, Detroit, 1988.

16. K. Takewaka and S. Mastumoto.. Quality and cover thickness of concrete based on the estimation of chloride penetration in Marine Environments. Second International Conference Concrete in Marine Environment Proceedings, St. Andrews by-the-Sea, Canada. ACI SP109-17, pp. 381-400. American Concrete Institute, Detroit, 1988.

17. T. Luping and L. Nilsson. (1993). Rapid Determination of the Chloride Diffusivity in concrete by applying an electrical field. ACI Materials Journal, Vol. 89, issue 1, pp. 49-53.

18. M. Manera, Ø. Vennesland, L. Bertolini. (2008). Chloride threshold for rebar corrosion in concrete with addition of silica fume. Corrosion Science, Vol. 50, issue 2, pp. 554-560.

19. L. Bertolini, F. Bolzoni, M. Gastaldi, T. Pastore, P. Pedeferri and E. Redaelli. (2009). Effects of cathodic prevention on the chloride threshold for steel corrosion in concrete. Electrochimica Acta, Vol. 54, pp. 1452-1463.

20. B.H. Oh, S.Y. Jang, Y.S. Shin. (2003). Experimental investigation of the threshold chloride concentration for corrosion initiation in reinforced concrete structures. Magazine of Concrete Research, Vol. 55, issue 2, pp. 117-124.

21. N.R. Buenfeld, G.K. Glass, A.M. Hassanein and J. Zhang. (1998). Chloride transport in concrete subjected to electric field. Journal of Materials in Civil Engineering, Vol. 10, issue 4, pp. 220-228.

22. L. Li and A.A.Sagüés. (2001). Chloride Corrosion Threshold of Reinforcing Steel in Alkaline Solutions - Open-Circuit Immersion Tests. Corrosion, Vol. 57, issue 1, pp. 19-28.

©2012 by NACE International. Requests for permission to publish this manuscript in any form, in part or in whole, must be in writing to NACE International, Publications Division, 1440 South Creek Drive, Houston, Texas 77084. The material presented and the views expressed in this paper are solely those of the author(s) and are not necessarily endorsed by the Association.